3. Results

3.1. Body and liver weights

Data for final body and liver weights in male and female *gpt* delta mice given DC are shown in Table 1. Although all of the values in DC-treated male mice were significantly lower than those in the controls, liver and relative liver weights in the treated female mice were significantly increased as compared with the controls.

3.2. In vivo mutation assays

Data for *gpt* MFs analyzed by 6-TG selection are summarized in Table 2. While there were no significant differences in the MFs between the male groups, the MF in the DC-treated females was 2.23 ± 0.55, which was significantly higher than the control value (0.48 ± 0.29). To characterize *gpt* mutations due to DC exposure, they were analyzed by DNA sequencing (Table 3). In the DC-treated female mice, G:C pairs were the preferred bases for mutation, accounting for 67.3% of the mutations (70/104). In the base substitutions, the predominant type was GC:TA (34/104, 32.7%) followed by GC:AT (26/104, 25.0%) and GC:CG (10/104, 9.6%). In addition, 16.3% (17/104) of mutant colonies were identified as carrying single- or multiple deletions. As shown in Table 4, Spi^- MFs in the treated male and female mice were not significantly different from those in the relevant controls.

Table 1
Body liver and relative liver weights of *gpt* delta mice given DC

Sex	Treatment	No. of mice	BW (g)	Liver (g)	Liver/BW (%)
Male	Control	5	32.6 ± 1.6	1.66 ± 0.21	5.07 ± 0.54
	Dicyclanil	5	29.0 ± 1.1**	1.42 ± 0.08*	4.89 ± 0.21*
Female	Control	5	25.0 ± 0.6	1.06 ± 0.05	4.25 ± 0.16
	Dicyclanil	5	24.0 ± 0.8	1.27 ± 0.07**	5.29 ± 0.12**

* $p < 0.05$ vs. Control.
** $p < 0.01$ vs. Control.

Table 2
gpt MFs in the livers of *gpt* delta mice given DC

Sex	Treatment	Animal No.	Cm^R colonies ($\times 10^5$)	6-TG^R and Cm^R colonies		Mutant frequency ($\times 10^{-6}$)	Mean ± S.D.
				Total	Independent		
Male	Control	1	9.0	6	5	0.56	0.42 ± 0.20
		2	10.7	7	7	0.66	
		3	6.9	4	3	0.44	
		4	9.5	4	3	0.31	
		5	12.4	2	2	0.16	
		6	11.5	6	5	0.43	
		7	10.7	1	1	0.09	
	Dicyclanil	8	8.9	8	8	0.90	0.48 ± 0.31
		9	6.1	4	4	0.66	
		10	9.7	3	3	0.31	
Female	Control	11	8.8	4	4	0.45	0.48 + 0.29
		12	6.5	5	2	0.31	
		13	12.6	2	2	0.16	
		14	7.6	7	7	0.93	
		15	8.7	5	5	0.57	
		16	7.0	31	19	2.72	
		17	13.0	29	26	2.01	
	Dicyclanil	18	11.1	51	25	2.26	2.23 ± 0.55*
		19	7.0	11	10	1.42	
		20	8.7	34	24	2.75	

* $p < 0.01$ vs. Control.

Table 3
Mutation spectra of *gpt* mutant colonies

Sex	Male				Female			
Treatment	Control		Dicyclanil		Control		Dicyclanil	
	Number (%)	MF ($\times 10^{-6}$)	Number (%)	MF ($\times 10^{-6}$)	Number (%)	MF ($\times 10^{-6}$)	Number (%)	MF ($\times 10^{-6}$)
Base substitutions								
Transversions								
GC:TA	1[a] (5.0)	0.02	1 (4.8)	0.02	1 (5.0)	0.02	34 (32.7)	0.73
GC:CG	3 (15.0)	0.06	3 (14.3)	0.07	1 (5.0)	0.02	10 (9.6)	0.21
AT:TA	1 (5.0)	0.02	3 (14.3)	0.07	1 (5.0)	0.02	10 (9.6)	0.21
AT:CG	0	0	0	0	2 (10.0)	0.05	2 (1.9)	0.04
Transitions								
GC:AT	6 (30.0)	0.13	11 (52.4)	0.25	5 (25.0)	0.12	26 (25.0)	0.56
AT:GC	3 (15.0)	0.06	1 (4.8)	0.02	3 (15.0)	0.07	0	0
Deletions								
Single bp	5 (25.0)	0.11	2 (9.5)	0.05	6 (30.0)	0.14	15 (14.4)	0.32
Over 2 bp	0	0	0	0	0	0	2 (1.9)	0.04
Insertions	1 (5.0)	0.02	0	0	1 (5.0)	0.02	1 (1.0)	0.02
Complexes	0	0	0	0	0	0	4 (3.8)	0.08
Total	20	0.42 ± 0.20	21	0.48 ± 0.31	20	0.48 ± 0.29	104	$2.23 \pm 0.55^{*}$

[a] The number of colonies with independent mutations.
* $p < 0.01$ vs. Control.

3.3. Oxidative DNA damage and lipid peroxidation

The results for 8-OHdG and TBARS in the livers of *gpt* delta mice given DC are illustrated in Figs. 2 and 3, respectively. 8-OHdG levels in the males and females (males; 0.62 ± 0.06, $p < 0.01$, females; 0.65 ± 0.13 8-OHdG/10^5dG, $p < 0.01$) treated with DC were elevated compared with the relevant control values (male;

Table 4
Spi^- MFs in the livers of *gpt* delta mice given DC

Sex	Treatment	Animal No.	Plaques within XL-1 Blue MRA ($\times 10^5$)	Plaques within XL-1 Blue MRA (P2) (Spi^-)	Mutant frequency (10^{-5})	Mean ± S.D.
Male	Control	1	10.4	4	0.39	0.27 ± 0.17
		2	13.3	2	0.15	
		3	19.4	3	0.16	
		4	14.2	2	0.14	
		5	11.7	6	0.51	
	Dicyclanil	6	20.4	10	0.49	0.42 ± 0.12
		7	17.1	4	0.23	
		8	10.1	4	0.40	
		9	12.5	7	0.56	
		10	11.6	5	0.43	
Female	Control	11	16.7	15	0.90	0.68 ± 0.29
		12	10.9	10	0.92	
		13	33.9	10	0.29	
		14	ND	ND	ND	
		15	19.4	12	0.62	
	Dicyclanil	16	18.9	14	0.74	0.83 ± 0.35
		17	22.6	29	1.28	
		18	17.4	7	0.40	
		19	15.4	10	0.65	
		20	16.0	17	1.06	

ND, not detected.

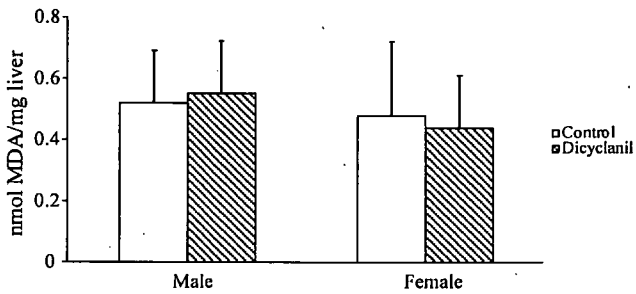

Fig. 2. Changes of TBARS levels in livers of male and female *gpt* delta mice fed DC in the diet at concentrations of 0 (Control) or 0.15% for 13 weeks. The values are means ± S.D.s of data for five animals.

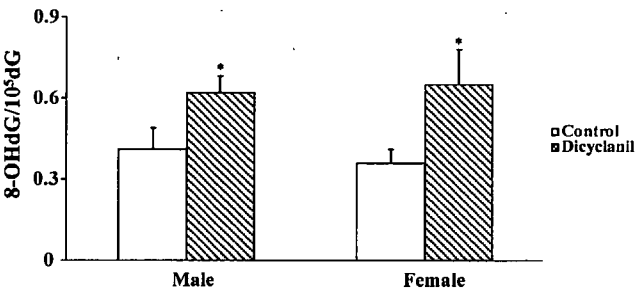

Fig. 3. Changes of 8-OHdG levels in liver nuclear DNA of male and female *gpt* delta mice fed DC in the diet at concentrations of 0 (Control) or 0.15% for 13 weeks. The values are means ± S.D.s of data for five animals. Significant differences from the relevant control are shown by $^{*}p < 0.01$.

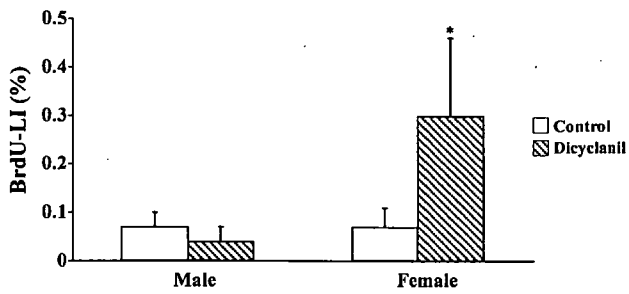

Fig. 5. Changes of BrdU-LIs in hepatocytes of male and female *gpt* delta mice fed DC at concentrations of 0 (Control) or 0.15% for 13 weeks. The values are means ± S.D.s of data for five animals. Significant differences from the relevant control are shown by $^{*}p < 0.05$.

0.41 ± 0.08, female; 0.36 ± 0.05 8-OHdG/10^5dG) with statistical significance. In contrast, there were no significant differences in TBARS levels among the groups.

3.4. Histopathology and immunohistochemical analysis of BrdU

Histopathologically, swelling of centrilobular hepatocytes was observed in the treated mice of both sexes without overt hepatocyte necrosis, the extents being almost equal in both genders (Fig. 4a and b). Fig. 5 summarizes changes in BrdU-LI for hepatocytes in male

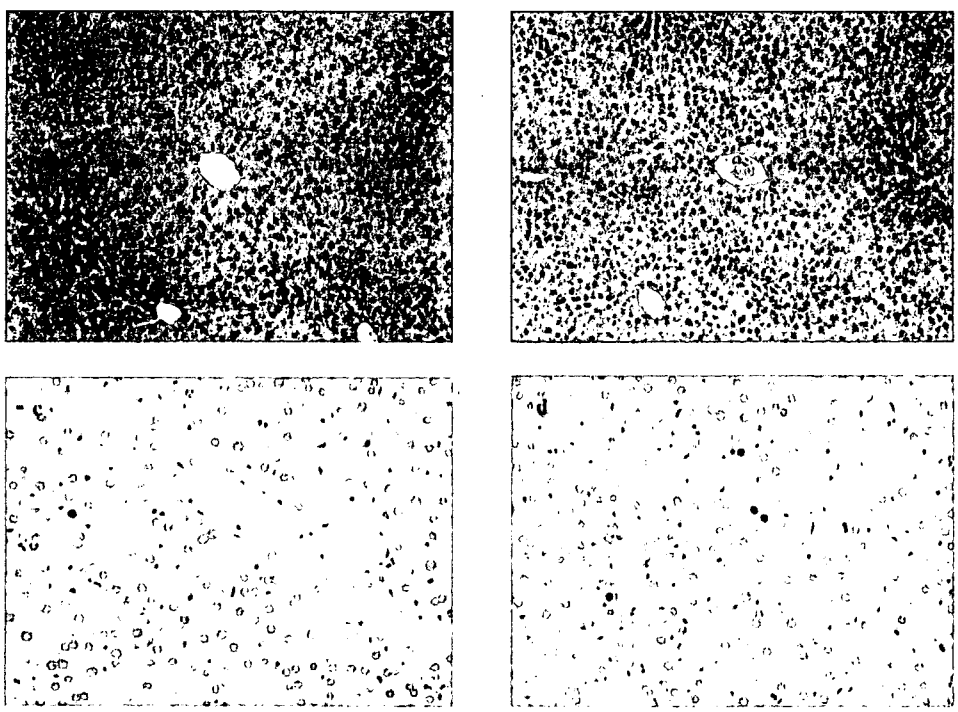

Fig. 4. Photomicrographs of livers of male (a and c) and female (b and d) *gpt* delta mice fed DC at a concentration of 0.15% for 13 weeks. Centrilobular hepatocyte hypertrophy is evident in both sexes (a and b). H&E staining at ×100 original magnification. In contrast to few BrdU-positive hepatocytes in a male (c), an appreciable number of the positive hepatocytes is evident in a female (d). BrdU immunohistochemical staining at ×200 original magnification.

and female *gpt* delta mice treated with DC. Although there were no differences between the male groups, BrdU-LIs in the treated females were elevated with significance ($0.30 \pm 0.17\%$, $p < 0.05$) as compared to the control value ($0.07 \pm 0.04\%$) (Fig. 4c and d).

4. Discussion

It has been reported that 18-month exposure of male and female mice to DC at a concentration of 0.15% in the diet caused hepatocelular adenomas and carcinomas with significantly elevated incidence only in the females, in spite of all negative outcomes in various genotoxicity studies [14]. In the present *in vivo* mutation assay, although there were no changes in Spi^- MFs, suggestive of large size of deletion mutations, among the groups, *gpt* MFs were significantly elevated in the females, but not the males. Their spectrum analyses revealed GC:TA transversion mutations to be predominant in the *gpt* mutations observed in the DC-treated females. To the best of our knowledge, this is the first report showing DC-induced genotoxicity, which was in good concordance with DC carcinogenicity in terms of the sex specificity.

It has been assumed that biotransformation of DC involves oxidative opening the cyclopropyl ring at various positions, followed by further oxidation and cleavage of the cyclopropyl-N-bond [14]. In the males, gene expression analysis using cDNA microarray and RT-PCR from the livers after DC treatment demonstrated upregulation of some metabolism-, reduction- and oxidation-related genes such as *CYP1A*, *Por* and *Txnrd 1*, suggesting a possible generation of reactive oxygen species (ROS) through P450-mediated metabolism of DC [22]. Hepatocyte hypertrophy was apparent in the treated mice of both genders and the present study revealed increases of 8-OHdG levels in liver DNA of female *gpt* delta mice given DC as well as the males, indicating that oxidative DNA damage due to ROS generated during DC metabolism is a phenomenon common to both sexes. By contrast, BrdU-LIs in hepatocytes were only significantly increased in the females, which were in line with the fact that significant increase in liver weights was observed in the treated females, but not the males. In the absence of overt cytotoxicity in the treated females, it seems unlikely that induction of cell proliferation resulted from a regenerative response, so that the underlying mechanisms remain unclear. It is well known that during cell replication, 8-OHdG primarily causes GC:TA transversion by mispairing with A bases [23,24]. Furthermore, the fact that regeneration of hepatocytes after partial hepatectomy does not affect 8-OHdG levels suggests that there is no replication coupled repair of preexisting 8-OHdG [25]. Consequently, high proliferation of cells with accumulated 8-OHdG lead to considerable increase in reporter gene MFs [25–27]. Accordingly, we hypothesized that the dual induction of 8-OHdG and cell proliferation due to DC exposure to female *gpt* delta mice might be responsible for the increment in the MFs. In addition, we have found that 4-week exposure of B6C3F1 mice, a back strain of *gpt* delta mice, to DC at the same dose was sufficient to induce significant elevation of 8-OHdG only in the females, but not the males, albeit without no overexpression of *OGG1*, *MYH* or *MTH* mRNA levels in the livers of both sexes (unpublished data). Therefore, it seems likely that the early onset of DNA oxidation is also responsible for the sex specificity.

As a matter of fact, 8-OHdG levels in nuclear genomic DNA may not always imply high levels of 8-OHdG at *gpt* loci specifically located at chromosome 17 [28]. It has been proposed that the distribution of 8-OHdG following exogenous oxidative stress is not random in the genome [29]. Nevertheless, abundant 8-OHdG modification at the *gpt* loci was reported to be observed in the kidneys of *gpt* delta mice treated with ferric nitrilotriacetate [30]. Partly due to the considerable number of copies of the transgene (approximately 80 copies) per haploid genome in the *gpt* delta mice [31], *gpt* loci indeed appear vulnerable to 8-OHdG modification [30]. Therefore, it is highly probable that DC exposure of the *gpt* delta mice caused accumulation of 8-OHdG at *gpt* loci judging from 8-OHdG levels in the genomic DNA. The present spectrum analysis of *gpt* mutants caused by DC exposure showed GC:AT transition mutations at the second highest incidence, despite this type of mutation being spontaneously observed with a certain incidence. In NIH3T3 cells transfected with the c-Ha-ras gene, which incorporates 8-OHdG at the first position of codon 12 (GGC), show mainly GC:TA transversions, while incorporation at the second position elicits GC:AT transitions to an appreciable extent [32,33]. In addition to our data, the results indicate that types of mutations other than GC:TA transversion mutations are induced by 8-OHdG in DNA [34]. We also found that 85.4% of base substitution mutations occurred at G:C pairs and 14.6% at A:T pairs. Although 1,N^6-ethenoadenosine formed during lipid peroxidation induces AT:GC transition mutations [35], this type of mutation was not evident among the *gpt* mutants. This might reflect the apparent lack of lipid peroxidation despite oxidative DNA damage due to DC treatment.

In conclusion, DC hitherto categorized as a non-genotoxic carcinogen was here shown to have the

potential to induce gene mutations at target site of DNA, possibly due to 8-OHdG formation. The co-examined data strongly suggest that induction of cell proliferation is required to predispose cells harboring high amounts of 8-OHdG to generation of mutations. Thus, the fact that DC-induced genotoxicity is dependent on cell proliferation in addition to nuclear DNA damage by ROS generated through DC metabolism might provide a reason for why genotoxicity has not been detected previously in various mutation assays. The overall data suggest that examination of several parameters associated with carcinogenesis using reporter gene transgenic rodents is a powerful tool for risk assessment of so-called non-genotoxic carcinogens.

Acknowledgements

We thank Ms. Machiko Maeda, Aki Kijima and Ayako Kaneko for expert technical assistance in carrying out the animal experiments and processing histological materials. This work was supported in part by a grant-in-aid for research on safety of veterinary drug residues in food of animal origin from the Ministry of Health, Labor and Welfare of Japan.

References

[1] P. Kasper, Y. Uno, R. Mauthe, N. Asano, G. Douglas, E. Matthews, M. Moore, L. Mueller, M. Nakajima, T. Singer, G. Speit, Follow-up testing of rodent carcinogens not positive in the standard genotoxicity testing battery: IWGT workgroup report, Mutat. Res. 627 (2007) 106–116.

[2] R.W. Tennant, M.R. Elwell, J.W. Spalding, R.A. Griesemer, Evidence that toxic injury is not always associated with induction of chemical carcinogenesis, Mol. Carcinog. 4 (1991) 420–440.

[3] G. Brambilla, A. Martelli, Failure of the standard battery of short-term tests in decting some rodent and human genotoxic carcinogens, Toxicology 196 (2004) 1–19.

[4] D. Kirkland, M. Aardema, L. Henderson, L. Muller, Evaluation of the ability of a battery of three in vitro genotoxicity tests to discriminate rodent carcinogens and non-carcinogens, I. Sensitivity, specificity and relative predictivity, Mutat. Res. 584 (2005) 1–256.

[5] T. Nohmi, T. Suzuki, K. Masumura, Recent advances in the protocols of transgenic mouse mutation assays, Mutat. Res. 455 (2000) 191–215.

[6] A. Nishikawa, T. Suzuki, M. Masumura, F. Furukawa, M. Miyauchi, H. Nakamura, H.-Y. Son, T. Nohmi, M. Hayashi, M. Hirose, Reporter gene transgenic mice as a tool for analyzing the molecular mechanisms underlying experimental carcinogenesis, J. Exp. Clin. Cancer Res. 20 (2001) 111–115.

[7] R. Schoeny, Use of genetic toxicology data in US EPA risk assessment: the mercury study report as an example, Environ. Health Perspect. 104 (Suppl. 3) (1996) 663–673.

[8] I.S. Pratt, T. Barron, Regulatory recognition of indirect genotoxicity mechanisms in the European Union, Toxicol. Lett. 140–141 (2003) 53–62.

[9] M.A. Pereira, W. Wang, P.M. Kramer, L. Tao, DNA hypomethylation induced by non-genotoxic carcinogens in mouse and rat colon, Cancer Lett. 212 (2004) 145–151.

[10] H.M. Bolt, H. Foth, J.G. Hengstler, G.H. Degen, Carcinogenicity categorization of chemicals-new aspects to be considered in a European perspective, Toxicol. Lett. 151 (2004) 29–41.

[11] M. Kirsch-Volders, A. Vanhauwaert, U. Eichenlaub-Ritter, I. Decordier, Indirect mechanisms of genotoxicity, Toxicol. Lett. 140–141 (2003) 63–74.

[12] K. Kanki, A. Nishikawa, K. Masumura, T. Umemura, T. Imazawa, Y. Kitamura, T. Nohmi, M. Hiorse, *In vivo* mutational analysis of liver DNA in *gpt* delta transgenic rats treated with the hepatocarcinogens *N*-nitrosopyrrolidine, 2-amino-3-methylimidazo[4,5-*f*]quinoline, and di(2-ethylhexyl)phthalate, Mol. Carcinog. 42 (2005) 9–17.

[13] Y. Kuroiwa, T. Umemura, A. Nishikawa, K. Kanki, Y. Ishii, Y. Kodama, K. Masumura, T. Nohmi, M. Hirose, Lack of *in vivo* mutagencity and oxidative DNA damage by flumequine in the livers of *gpt* delta mice, Arch. Toxicol. 81 (2007) 63–69.

[14] WHO, Toxicological evaluation of certain veterinary drug residues in food, fifty-fourth meeting of the Joint FAO/WHO Expert Committee on Food Additives, WHO Food Additive Ser. 45 (2000) 75–89.

[15] M. Moto, Y.F. Sasaki, M. Okamura, M. Fujita, Y. Kashida, N. Machida, K. Mitsumori, Absence of *in vivo* genotoxicity and liver initiation activity of dicyclanil, J. Toxicol. Sci. 28 (2003) 173–179.

[16] M. Moto, T. Umemura, M. Okamura, M. Muguruma, T. Ito, M. Jin, Y. Kashida, K. Mitsumori, Possible involvement of oxidative stress in dicyclanil-induced hepatocarcinogenesis in mice, Arch. Toxicol. 80 (2006) 694–702.

[17] T. Umemura, K. Tokumo, G.M. Williams, Cell proliferation induced in the kidneys and livers of rats and mice by short term exposure to the carcinogen *p*-dichlorobenzene, Arch. Toxicol. 66 (1992) 503–507.

[18] H. Kasai, Chemistry-based studies on oxidative DNA damage: formation, repair, and mutagenesis, Free Rad. Biol. Med. 33 (2002) 450–456.

[19] D. Nakae, Y. Mizumoto, E. Kobayashi, O. Noguchi, Y. Konishi, Improved genomic/nuclear DNA extraction for 8-hydroxydeoxyguanosine analysis of small amounts of rat liver tissue, Cancer Lett. 87 (1995) 233–239.

[20] H.J. Helbock, K.B. Beckman, M.K. Shigenaga, P.B. Walter, A.A. Woodall, H.C. Yeo, B.N. Ames, DNA oxidation matters: the HPLC-electrochemical detection assay of 8-oxo-deoxyguanosine and 8-oxo-guanine, Proc. Natl. Acad. Sci. U.S.A. 95 (1998) 288–293.

[21] M. Uchiyama, M. Mihara, Determination of malondialdehyde precursor in tissue by the thiobarbituric acid test, Anal. Biochem. 86 (1978) 271–278.

[22] M. Moto, M. Okamura, T. Muto, Y. Kashida, N. Machida, K. Mitsumori, Molecular pathological analysis on the mechanism of liver carcinogenesis in dicyclanil-treated mice, Toxicology 207 (2005) 419–436.

[23] K.C. Cheng, D.S. Cahill, H. Kasai, S. Nishimura, L.A. Loeb, 8-Hydroxyguanine, an abundant form of oxidative DNA damage, causes G → T and A → C substitutions, J. Biol. Chem. 267 (1992) 166–172.

[24] S. Shibutani, M. Takeshita, A.P. Grollman, Insertion of specific bases during DNA synthesis past the oxidation damaged base 8-oxodG, Nature 191 (1991) 431–434.

[25] T. Arai, V.P. Kelly, K. Komoro, O. Minowa, T. Noda, S. Nishimura, Cell proliferation in liver of *Mmh/Ogg1*-deficient

mice enhances mutation frequency because of the presence of 8-hydroxyguanine in DNA, Cancer Res. 63 (2003) 4287–4292.
[26] T. Arai, V.P. Kelly, O. Minowa, T. Noda, S. Nishimura, High accumulation of oxidative DNA damage, 8-hydroxyguanosine, in *Mmh/Ogg1* deficient mice by chronic oxidative stress, Carcinogenesis 23 (2002) 2005–2010.
[27] T. Umemura, K. Kanki, Y. Kuroiwa, Y. Ishii, K. Okano, T. Nohmi, A. Nishikawa, M. Hirose, *In vivo* mutagenicity and initiation following oxidative DNA lesions in the kidneys of rats given potassium bromate, Cancer Sci. 97 (2006) 829–835.
[28] K. Masumura, M. Matsui, M. Katoh, N. Horiya, O. Ueda, H. Tanabe, M. yamada, H. Suzuki, T. Fofuni, T. Nohmi, Spectra of *gpt* mutations in ethylnitrosourea-treated and untreated transgenic mice, Environ. Mol. Mutagen. 34 (1999) 1–8.
[29] S. Akatsuka, T.T. Aung, K.K. Dutta, L. Jiang, W.-H. Lee, Y.-T. Liu, J. Onuki, T. Shirase, K. Yamasaki, H. Ochi, Y. naito, T. Yoshikawa, H. Kasai, Y. Tominaga, K. sakumi, Y. Nakabeppu, Y. Kawai, K. Uchida, A. Yamasaki, T. Tsuruya, Y. Yamada, S. Toyokuni, Contrasting genome-wide distribution of 8-hydroxyguanine and acrolein-modified adenine during oxidative stress-induced renal carcinogenesis, Am. J. Pathol. 169 (2006) 1328–1342.
[30] L. Jiang, Y. Zhong, S. Akatsuka, Y.-T. Liu, K. Dutta, W.-H. Lee, J. Onuki, K. Masumura, T. Nohmi, S. Toyokuni, Deletion and single nucleotide substitution at G:C in the kidney of *gpt* delta transgenic mice after ferric nitrilotriacetate treatment, Cancer Sci. 97 (2006) 1159–1167.
[31] T. Nohmi, M. Katoh, H. Suzuki, M. Matsui, M. Yamada, M. Watanabe, M. Suzuki, N. Horiya, O. Ueda, T. Shibuya, H. Ikeda, T. Sofuni, A new transgenic mouse mutagenesis test system using Spi$^-$ and 6-thioguanine selections, Environ. Mol. Mutagen. 28 (1996) 465–470.
[32] H. Kamiya, K. Miura, H. Ishikawa, H. Inoue, S. Nishimura, E. Ohtsuka, c-Ha-*ras* containing 8-hydroxyguanine at codon 12 induces point mutations at the modified and adjacent position, Cancer Res. 52 (1992) 3483–3485.
[33] P. Jaloszynski, C. Masutani, F. Hanaoka, A.B. Perez, S. Nishimura, 8-Hydroxyguanine in a mutational hotspot of the c-Ha-*ras* gene causes misreplication, action-at-a-distance mutagenesis and inhibition of replication, Nucleic Acid Res. 21 (2003) 6085–6095.
[34] S. Nishimura, Involvement of mammalian OGG1 (MMH) in excision of the 8-hydroxyguanine residue in DNA, Free Rad. Biol. Med. 32 (2002) 813–821.
[35] G.A. Padya, M. Moriya, 1,N^6-ethenodeoxyadenosine, a DNA adduct highly mutagenic in mammalian cells, Biochemistry 35 (1996) 11487–11492.

Available online at www.sciencedirect.com
ScienceDirect
Mutation Research 626 (2007) 15–25
Genetic Toxicology and Environmental Mutagenesis
www.elsevier.com/locate/gentox
Community address: www.elsevier.com/locate/mutres

Combined genotoxic effects of radiation and a tobacco-specific nitrosamine in the lung of *gpt* delta transgenic mice

Megumi Ikeda[a,b], Ken-ichi Masumura[a], Yasuteru Sakamoto[a], Bing Wang[c], Mitsuru Nenoi[c], Keiko Sakuma[b], Isamu Hayata[c], Takehiko Nohmi[a,*]

[a] *Division of Genetics and Mutagenesis, National Institute of Health Sciences, 1-18-1 Kamiyoga, Setagaya-ku, Tokyo 158-8501, Japan*
[b] *Graduate School of Nutrition and Health Sciences, Kagawa Nutrition University, 3-9-21 Chiyoda, Sakado-shi, Saitama 350-0288, Japan*
[c] *Radiation Effect Mechanisms Research Group, Research Center of Radiation Protection, National Institute of Radiological Sciences, 4-9-1 Anagawa, Inage-ku, Chiba-shi, Chiba 263-8555, Japan*

Received 22 May 2006; received in revised form 25 July 2006; accepted 31 July 2006
Available online 7 September 2006

Abstract

It is important to evaluate the health effects of low-dose-rate or low-dose radiation in combination with chemicals as humans are exposed to a variety of chemical agents. Here, we examined combined genotoxic effects of low-dose-rate radiation and 4-(methylnitrosamino)-1-(3-pyridyl)-1-butanone (NNK), the most carcinogenic tobacco-specific nitrosamine, in the lung of *gpt* delta transgenic mice. In this mouse model, base substitutions and deletions can be separately analyzed by *gpt* and Spi$^-$ selections, respectively. Female *gpt* delta mice were either treated with γ-irradiation alone at a dose rate of 0.5, 1.0 or 1.5 mGy/h for 22 h/day for 31 days or combined with NNK treatments at a dose of 2 mg/mouse/day, i.p. for four consecutive days in the middle course of irradiation. In the *gpt* selection, the NNK treatments enhanced the mutation frequencies (MFs) significantly, but no obvious combined effects of γ-irradiation were observable at any given radiation dose. In contrast, NNK treatments appeared to suppress the Spi$^-$ large deletions. In the Spi$^-$ selection, the MFs of deletions more than 1 kb in size increased in a dose-dependent manner. When NNK treatments were combined, the dose–response curve became bell-shaped where the MF at the highest radiation dose decreased substantially. These results suggest that NNK treatments may elicit an adaptive response that eliminates cells bearing radiation-induced double-strand breaks in DNA. Possible mechanisms underlying the combined genotoxicity of radiation and NNK are discussed, and the importance of evaluation of combined genotoxicity of more than one agent is emphasized.

Keywords: Combined genotoxic effects; Radiation; NNK; Lung cancer; *gpt* delta mice; Deletion

1. Introduction

Environmental factors play important roles in the etiology of human cancer [1]. Of various environmental hazardous compounds, cigarette smoke is the most causative factor associated with the increase in cancer risk in humans. Tobacco smoking plays a major role in the etiology of lung, oral cavity and esophageal cancers, and a variety of chronic degenerative diseases [2]. Although cigarette smoke is a mixture of about 4000 chemicals including more than 60 known human carcinogens, 4-(methylnitrosamino)-1-(3-pyridyl)-1-butanone (nicotine-derived nitrosamino ketone, NNK) is the most carcinogenic tobacco-specific nitrosamine [3,4]. NNK induces lung tumors in mice,

* Corresponding author. Tel.: +81 3 3700 9873; fax: +81 3 3707 6950.
E-mail address: nohmi@nihs.go.jp (T. Nohmi).

1383-5718/$ – see front matter © 2006 Elsevier B.V. All rights reserved.
doi:10.1016/j.mrgentox.2006.07.003

rats and hamsters, and International Agency for Research on Cancer has concluded that exposure to NNK and NNN (*N'*-nitrosonornicotine) is carcinogenic to humans [5]. NNK is metabolically activated by CYP (P-450) enzymes in the lung and generates O^6-methylguanine in DNA, which leads to G:C to A:T mutations, and the subsequent activation of Ki-*ras* proto-oncogene, an initiation of tumor development [6,7].

Radiation, on the other hand, is one of the most causative physical factors that induce human cancer. Radiation induces double-strand breaks (DSBs) in DNA, which lead to chromosome aberrations and cell deaths, and generates a variety of oxidative DNA damage [8]. Because of the genotoxicity, radiation at high doses clearly induces various tumors in humans [9]. Even at low doses, residential exposure to radioactive radon and its decay products may account for about 10% of all lung cancer deaths in the United States and about 20% of the lung cancer cases in Sweden [10,11].

Since humans are exposed to a variety of chemical and physical agents that may induce cancer, these factors may interact with each other and the action of one agent may be influenced by exposure to another agent [12]. The risk from combined exposure to more than one agent may be substantially higher or lower than predicted from the sum of the individual agents. In fact, low-dose radiation can induce an adaptive response, causing rodent or human cells to become resistant to genotoxic damage by subsequent higher doses of radiation [13]. Pre-exposure to alkylating agents at low doses induces another adaptive response that provides mechanisms by which the exposed bacterial cells can tolerate the higher challenging doses of genotoxic agents [14]. In addition, mitomycin C, bleomycin, hydrogen peroxide, metals and quercetin may also induce an adaptive response [15].

To explore the mechanisms underlying the interactive effects of chemical and physical agents on carcinogenesis, we examined the combined genotoxic effects of NNK and γ-irradiation in the lung of *gpt* delta transgenic mice [16]. In this mouse model, point mutations and deletions are separately analyzable by *gpt* and Spi^- selections, respectively [17]. Point mutations such as base substitutions are induced by a number of chemical carcinogens including NNK [18]. Spi^- selection detects deletions in size between 1 bp and 10 kb [19]. Deletions in size more than 1 kb, which we call large deletions in this study, are efficiently induced by γ-ray, X-ray and carbon-ion irradiation [20], and are thought to be generated by non-homologous end joining (NHEJ) of DSBs in DNA [21].

We report here that low-dose-rate γ-irradiation enhanced the mutation frequencies (MFs) of the large deletions in the lung of *gpt* delta mice in a dose-dependent manner. When combined with NNK treatments, however, the MF at the highest radiation dose, i.e., 1.02 Gy, was reduced by more than 50%, suggesting that NNK treatments may induce an adaptive response against radiation-induced deletion mutations. We discuss possible mechanisms of the adaptive response and emphasize the importance of the risk assessment of combined genotoxic effects of radiation and chemicals in vivo.

2. Materials and methods

2.1. Treatment of mice

gpt delta C57BL/6J transgenic mice were maintained in the conventional animal facility of National Institute of Radiological Sciences, Chiba, Japan, according to the institutional animal care guidelines. They were housed in autoclaved aluminum cages with sterile wood chips for bedding and given free access to standard laboratory chow (MB-1, Funabashi Farm Co., Japan) and acidified water under controlled lighting (12 h light/dark cycle). Seven-week-old female *gpt* delta mice were divided to eight groups each consisting of six mice. Three groups were γ-irradiated at a dose rate of 0.5, 1.0 or 1.5 mGy/h for 22 h/day for 2 weeks (Fig. 1). After the irradiation, three groups of mice were treated with a single i.p. injection of NNK (Toronto Research Chemicals, Toronto, Canada) dissolved in saline at a daily dose of 2 mg/mouse for four consecutive days. The irradiation continued during the 4-day treatments, and the mice were kept in the cage for another 2 weeks with irradiation. Three control groups were γ-irradiated as described but received saline instead of NNK. The whole irradiation period was 31 days, and the total estimated doses were 0.34, 0.68 and 1.02 Gy, respectively. Another control group of mice was treated with NNK as described but without γ-irradiation. The third control was kept in the cage for 31 days without γ-irradiation or NNK treatments. The source of radiation was ^{137}Cs, and the dose rate was estimated by a fluorescent glass dosimeter. The non-irradiated control groups were placed behind a concrete wall of 1 m thickness. The mice were sacrificed by cervical vertebral dislocation. The liver and lung were removed, placed immediately in liquid nitrogen, and stored at −80 °C until analysis.

2.2. DNA isolation and in vitro packaging of DNA

High-molecular-weight genomic DNA was extracted from the lung and the liver using the RecoverEase DNA Isolation Kit (Stratagene, La Jolla, CA). Lambda EG10 phages were rescued using Transpack Packaging Extract (Stratagene, La Jolla, CA).

2.3. gpt mutation assay

The *gpt* mutagenesis assay was performed according to previously described methods [17]. Briefly, *Escherichia coli*

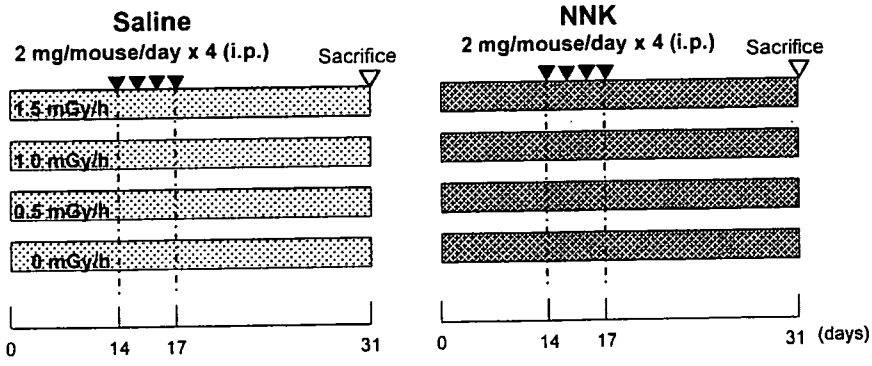

Fig. 1. An experimental design to examine the combined genotoxicity of γ-irradiation and NNK treatments in the lung of mice. Female 7-week-old *gpt* delta mice were divided into eight groups each composed of six mice. Three groups of mice were irradiated at a dose rate of 0.5, 1.0 or 1.5 mGy/h for 22 h/day for 14 days and treated with NNK at a daily dose of 2 mg/mouse for four consecutive days. The irradiation continued during the NNK treatments and the following 14 days before sacrifice. The total radiation doses were 0.34, 0.68 and 1.02 Gy, respectively. Control three groups of mice were γ-irradiated but without NNK treatments. Another control group was treated with NNK but without γ-irradiation. The third control was kept in the cage for 31 days without γ-irradiation or NNK treatments. Transgene λEG10 DNA was rescued from the lung of mice, and the base substitutions and deletions were analyzed by *gpt* and Spi$^-$ selection, respectively.

YG6020 expressing Cre recombinase was infected with the rescued phage. The bacteria were then spread onto M9 salts plates containing chloramphenicol (Cm) and 6-thioguanien (6-TG), and incubated for 72 h at 37 °C for selection for the colonies harboring a plasmid carrying the Cm acetyltransferase (*cat*) gene and a mutated *gpt* gene. The 6-TG-resistant colonies were streaked again onto the same selection plates for confirmation of the resistant phenotype. All the confirmed *gpt* mutants recovered from the lung were sequenced and the identical mutations from the same mouse counted one mutant. The *gpt* MFs in the lung were calculated by dividing the number of the *gpt* mutants after sequencing by the number of rescued plasmids, which was estimated from the number of colonies on plates containing Cm but without 6-TG. Since no *gpt* mutants recovered from the liver were sequenced, the MFs in the liver were calculated by dividing the number of confirmed 6-TG-resistant colonies by the number of rescued plasmids.

2.4. PCR and DNA sequencing analysis of 6-TG-resistant mutants

A 739 bp DNA fragment containing the *gpt* gene was amplified by polymerase chain reaction (PCR) using primers 1 and 2 [17]. The reaction mixture contained 5 pmol of each primer and 200 mM of each dNTP. PCR amplification was carried out using Ex Taq DNA polymerase (Takara Bio, Shiga, Japan) and performed with a Model PTC-200 Thermal Cycler (MJ Research, Waltham, MA). PCR products were analyzed by agarose gel electrophoresis to determine the amount of the products. DNA sequencing of the *gpt* gene was performed with BigDye™ Terminator Cycle Sequencing Kit (Applied Biosystems, Foster City, CA) using sequencing primer gptA2 (5′-TCTCGCGCAACCTATTTTCCC-3′). The sequencing reaction products were analyzed on an Applied Biosystems model 310 genetic analyzer (Applied Biosystems, Foster City, CA).

2.5. Spi$^-$ mutation assay

The Spi$^-$ assay was performed as described previously [17]. The lysates of Spi$^-$ mutants were obtained by infection of *E. coli* LE392 with the recovered Spi$^-$ mutants. The lysates were used as templates for PCR analysis to determine the deleted regions. Sequence changes in the *gam* and *redAB* genes, and the outside of the *gam/redAB* genes were identified by DNA sequencing analysis [22]. The appropriate primers for DNA sequencing were selected based on the results of PCR analysis. The entire sequence of λEG10 is available at http://dgm2alpha.nhis.go.jp.

2.6. Statistical analysis

All data are expressed as mean ± standard deviations of the MFs of six mice for lung and those of four mice for liver. Differences between groups were tested for statistical significance using a Student's *t*-test. A p value less than 0.05 denoted the presence of a statistically significant difference.

3. Result

3.1. gpt MFs in the lung of NNK-treated and γ-irradiated gpt delta mice

We measured the *gpt* MFs in the lung of *gpt* delta mice untreated or treated with NNK in the absence or the presence of γ-irradiation (Fig. 2). NNK treatments significantly enhanced the MFs over the control groups. The mean MFs ($\times 10^{-6}$) of NNK-treated versus saline-treated groups were 14.3 ± 6.9 versus 4.2 ± 4.0, 20.7 ± 5.1 versus 4.7 ± 3.0, 15.2 ± 7.3 versus 2.0 ± 2.1 and 17.2 ± 7.9 versus 2.7 ± 1.4 at the dose rates of 0, 0.5, 1.0 and 1.5 mGy/h, respectively. The γ-irradiation

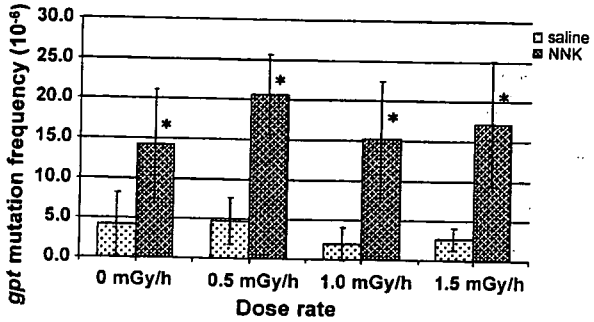

Fig. 2. *gpt* MFs in the lung of mice untreated or treated with NNK in the absence or the presence of γ-irradiation. An asterisk (*) denotes $p < 0.05$ ($n = 6$) in a Student's *t*-test of MF of NNK-treated vs. the corresponding untreated mice. Vertical bars show the standard deviations with mice as the unit of comparison.

alone, i.e., the saline-treated group, did not enhance the *gpt* MF under the conditions. Hence, the increases in MFs are due to NNK treatments. Although the individual MFs slightly varied, there was no significant difference among the four MFs of the NNK-treated groups. Thus, we suggested that the irradiation did not modify the genotoxicity of NNK in the lung of mice.

To confirm the results in the lung, we analyzed the *gpt* MFs in the liver of the NNK-treated and saline-treated groups. The mean MFs ($\times 10^{-6}$) of NNK-treated versus saline-treated groups were 134 ± 48 versus 8.1 ± 3.8, 105 ± 31 versus 8.7 ± 3.5, 101 ± 18 versus 8.0 ± 4.2 and 128 ± 76 versus 6.8 ± 0.6 at the dose rates of 0, 0.5, 1.0 and 1.5 mGy/h, respectively. Although NNK treatments induced mutations much more strongly in the liver than in the lung, there were no significant modulating effects of radiation on the NNK-induced mutations in the liver.

The irradiation might modulate specific types of mutations without affecting the total *gpt* MFs. To examine the possibility, we determined the mutation spectra of the *gpt* gene in the lung and examined whether the radiation affected specific types of mutations (Table 1). NNK treatments induced G:C to A:T, G:C to T:A, A:T to T:A and A:T to C:G mutations. In particular, A:T to T:A mutations were induced more than 20-fold by NNK treatments. We observed, however, no remarkable variations of mutation spectra associated with the dose rates of combined radiation. Thus, we concluded that the irradiation did not enhance or suppress the base substitutions induced by NNK in the lung of *gpt* delta mice significantly.

3.2. *Spi⁻ MFs in the lung of NNK-treated and γ-irradiated gpt delta mice*

Next, we measured the Spi⁻ MFs in the lung of *gpt* delta mice untreated or treated with NNK in the absence or the presence of γ-irradiation. The mean Spi⁻ MFs ($\times 10^{-6}$) of NNK-treated versus saline-treated groups were 5.15 ± 2.34 versus 4.11 ± 0.98, 5.47 ± 1.98 versus 5.06 ± 3.50, 5.36 ± 1.56 versus 4.09 ± 0.80 and 5.39 ± 2.56 versus 4.65 ± 1.78 at the dose rates of 0, 0.5, 1.0 and 1.5 mGy/h, respectively. These results suggest that neither NNK treatments nor the irradiation enhanced the Spi⁻ MFs in the lung significantly.

To investigate the combined effects of NNK and γ-irradiation on specific types of deletion mutations, we identified all the Spi⁻ mutations by DNA sequencing analysis (Table 2). Of various classes of deletions observed, only the MFs of large deletions in the size of more 1 kb increased in a dose-dependent manner in the saline-treated group. To examine the dose–response in more detail, we determined the MFs of the large deletions

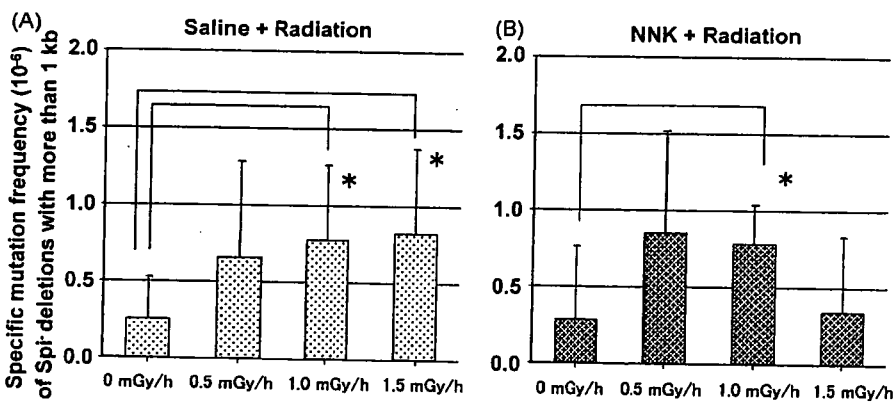

Fig. 3. Specific MF of large deletions with the size of more than 1 kb in the lung of unirradiated or γ-irradiated mice. The mice were not treated (A) or treated with NNK (B). An asterisk (*) denotes $p < 0.05$ ($n = 5$) in a Student's *t*-test of MF of γ-irradiated vs. the corresponding unirradiated mice. Vertical bars show the standard deviations with mice as the unit of comparison.

Table 1
gpt mutation spectra in the lung of NNK-treated and γ-irradiated *gpt* delta mice

Treatment: saline	0 mGy/h			0.5 mGy/h			1.0 mGy/h			1.5 mGy/h		
	No.	MF ($\times 10^{-6}$)	%	No.	MF ($\times 10^{-6}$)	%	No.	MF ($\times 10^{-6}$)	%	No.	MF ($\times 10^{-6}$)	%
Base substitution												
Transition												
G:C → A:T	15(6)	1.81	43	12(6)	1.76	38	5(2)	0.61	29	8(4)	0.81	30
A:T → G:C	2	0.24	6	4	0.59	13	1	0.12	6	2	0.20	7
Transversion												
G:C → T:A	1	0.12	3	5(2)	0.73	16	1	0.12	6	6(1)	0.61	22
G:C → C:G	1	0.12	3	0	0.00	0	0	0.00	0	2(2)	0.20	7
A:T → T:A	1	0.12	3	1	0.15	3	1	0.12	6	1	0.10	4
A:T → C:G	3	0.36	9	1	0.15	3	1	0.12	6	1	0.10	4
Deletion	8	0.97	23	6	0.88	19	7	0.85	41	6	0.61	22
−1 bp	3			2			5			3		
>2 bp	5			4			2			3		
Insertion	3	0.36	9	3	0.44	9	1	0.12	6	1	0.10	4
Others	1	0.12	3	0	0.00	0	0	0.00	0	0	0.00	0
	35	4.23	100	32	4.69	100	17	2.06	100	27	2.73	100

Treatment: NNK	0 mGy/h			0.5 mGy/h			1.0 mGy/h			1.5 mGy/h		
	No.	MF ($\times 10^{-6}$)	%	No.	MF ($\times 10^{-6}$)	%	No.	MF ($\times 10^{-6}$)	%	No.	MF ($\times 10^{-6}$)	%
Base substitution												
Transition												
G:C → A:T	24(2)	5.11	36	45(8)	8.02	39	32(5)	5.85	39	54(6)	8.51	50
A:T → G:C	0	0.00	0	7	1.25	6	6	1.10	7	2	0.32	2
Transversion												
G:C → T:A	9(2)	1.92	13	10(1)	1.78	9	7(1)	1.28	8	7(1)	1.10	6
G:C → C:G	0	0.00	0	2	0.36	2	0	0.00	0	3	0.47	3
A:T → T:A	13	2.77	19	26	4.64	22	17	3.11	21	17(1)	2.68	16
A:T → C:G	15	3.19	22	12	2.14	10	8	1.46	10	12(1)	1.89	11
Deletion	5	1.06	8	12	2.14	10	9	1.65	11	12	1.89	11
−1 bp	5			6			4			5		
>2 bp	0			6			5			7		
Insertion	1	0.21	2	0	0.00	0	4	0.73	5	1	0.16	1
Others	0	0.00	0	2	0.36	2	0	0.00	0	1	0.16	1
	67	14.26	100	116	20.68	100	83	15.18	100	109	17.18	100

No. stands for the number of mutations.

of each mouse and calculated the mean MF and standard derivations. The mean MFs ($\times 10^{-6}$) and standard derivations were 0.25 ± 0.28, 0.66 ± 0.63, 0.77 ± 0.49 and 0.82 ± 0.55 at the dose rates of 0, 0.5, 1.0 and 1.5 mGy/h, respectively (Fig. 3A). The values at 1.0 and 1.5 mGy/h were about three-fold higher than the value at 0 mGy/h, and the differences were statistically significant ($p = 0.04$). In contrast, the dose–response curve of large deletions in NNK-treated group was a bell shaped (Fig. 3B). The mean MFs ($\times 10^{-6}$) and standard derivations of large deletions in the NNK-treated group were 0.29 ± 0.47, 0.85 ± 0.66, 0.78 ± 0.26 and 0.35 ± 0.48 at the dose rates of 0, 0.5, 1.0 and 1.5 mGy/h, respectively. It should be noted that the

Table 2
Spi⁻ mutation spectra in the lung of NNK-treated and γ- irradiated *gpt* delta mice

Treatment: saline	0 mGy/h			0.5 mGy/h			1.0 mGy/h			1.5 mGy/h		
	No.	MF ($\times 10^{-6}$)	%	No.	MF ($\times 10^{-6}$)	%	No.	MF ($\times 10^{-6}$)	%	No.	MF ($\times 10^{-6}$)	%
1 bp deletion												
Simple												
Guanine	9	0.49	12	7	0.59	12	5	0.34	8	4	0.30	7
Adenine	4	0.22	5	0	0.00	0	2	0.14	3	1	0.08	2
In run												
Guanine	13	0.71	17	15	1.27	25	12	0.82	20	13	0.99	21
Adenine	31	1.70	41	19	1.60	32	22	1.50	37	25	1.91	41
With b.s.	0	0.00	0	0	0.00	0	0	0.00	0	0	0.00	0
>2 bp deletion	15	0.82	20	17	1.43	28	17	1.16	28	13	0.99	21
2 bp ~ 1 kb	2	0.11	3	7	0.59	12	3	0.20	5	1	0.08	2
>1 kb	5	*0.27*	7	7	*0.59*	12	11	*0.75*	18	10	*0.76*	16
Complex	8	0.44	11	3	0.25	5	3	0.20	5	2	0.15	3
Insertion	3	0.16	4	2	0.17	3	2	0.14	2	5	0.38	8
	75	4.11	100	60	5.06	100	60	4.09	100	61	4.65	100

Treatment: NNK	0 mGy/h			0.5 mGy/h			1.0 mGy/h			1.5 mGy/h		
	No.	MF ($\times 10^{-6}$)	%	No.	MF ($\times 10^{-6}$)	%	No.	MF ($\times 10^{-6}$)	%	No.	MF ($\times 10^{-6}$)	%
1 bp deletion												
Simple												
Guanine	5	0.61	12	4	0.46	8	4	0.50	9	4	0.48	9
Adenine	3	0.37	7	0	0.00	0	4	0.50	9	1	0.12	2
In run												
Guanine	9	1.10	21	19	2.17	40	9	1.12	21	14	1.68	31
Adenine	12	1.47	29	10	1.14	21	9	1.12	21	15	1.80	33
With b.s.	0	0.00	0	0	0.00	0	2	0.25	5	0	0.00	0
>2 bp deletion	12	1.47	29	10	1.14	21	11	1.37	26	11	1.32	24
2 bp ~ 1 kb	6	0.74	14	2	0.23	4	3	0.37	7	7	0.84	16
>1 kb	2	*0.25*	5	7	*0.80*	15	7	*0.87*	16	2	*0.24*	4
Complex	4	0.49	10	1	0.11	2	1	0.12	2	2	0.24	4
Insertion	1	0.12	2	5	0.57	10	4	0.50	9	0	0.00	0
	42	5.15	100	48	5.47	100	43	5.36	100	45	5.39	100

No. stands for the number of mutations. Specific MFs of large deletions more than 1 kb in size are italicised.

MF at 1.0 mGy/h (0.78×10^{-6}) was about three-fold higher than that of 0 mGy/h ($p = 0.04$) but the MF at 1.5 mGy/h (0.35×10^{-6}) was very similar to that of 0 mGy/h (0.29×10^{-6}). The p values of the differences of MFs between saline-treated and NNK-treated groups at dose rates of 0, 0.5, 1.0 and 1.5 mGy/h were 0.44, 0.32, 0.48 and 0.09, respectively. From the results, we suggested that NNK treatments suppressed the induc-

Fig. 4. Molecular nature of large deletions recovered from the lung of *gpt* delta mice untreated or treated with NNK in the absence or the presence of γ-irradiation. Horizontal bars represent the deleted regions of mutants. Most of the mutants lack the entire *gam* gene and part of the *redAB* genes, but some lack the *gam* gene and the upstream region. The *gam* and *redAB* genes make an operon and the transcription starts from the upstream of the *gam* gene. Short homologous sequences in the junctions of the mutants are underlined. Underlined sequences, i.e., T or CTTA, in the middle of two sequences are inserted sequences in the junctions.

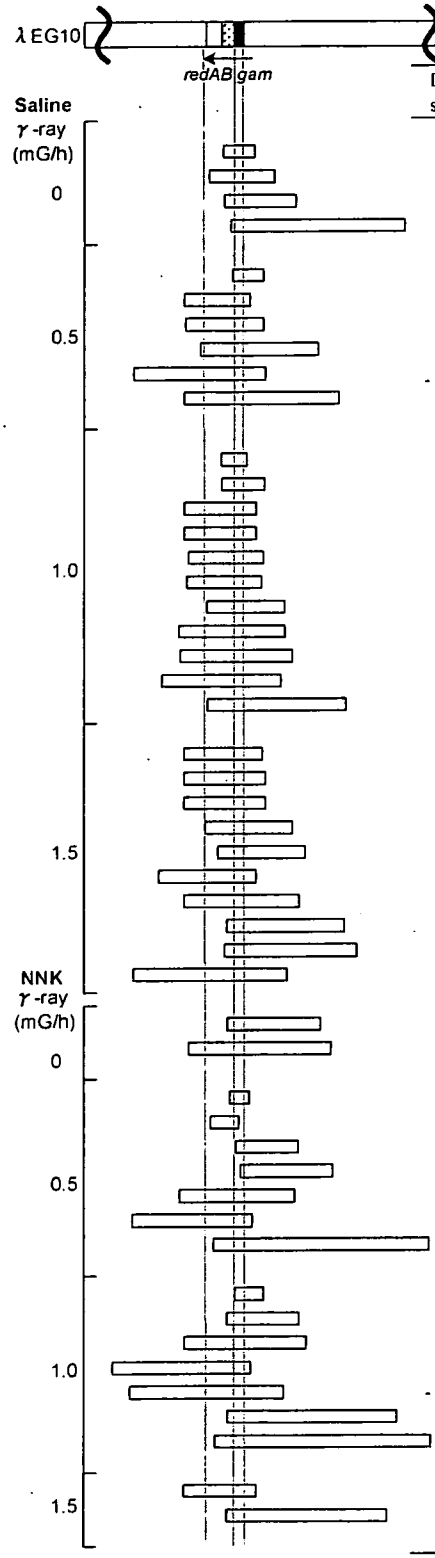

Delesion size (bp)	Sequence of the junction of deletion		No.of mutant	Mouse I.D.
- 1242	TGAATGGTTCGCGGCGGC	GTGTTTGTGCATCCATCT	2	2,34
- 2912	AGAGCAGGCGGTACGCAT	TAATCCTTAACTTTGCCC	1	34
- 3393	GGTAAATCCGGCATGTAC	AGCCAGGGGATCTCTCCC	1	34
- 7626	CAGCCAGCGTTGCGAGTG	CGGTTGCTTTATGCATGG	1	3
- 1608	GCTATCACGTTGTGAACT	TCGGATTTAGTGCGCTTT	2	9,11
- 2912	AGAGCAGGCGGTACGCAT	TAATCCTTAACTTTGCCC	1	9
- 3650	ACTGTTGGTTAATACGCT	AAAGCTCCAAGCTCAACA	1	41
- 5339	GATGCGGCTAACGTATGA	TGCCTTTGCGGCTTGTAA	1	11
- 5582 + 1	CGCCTGTCTCTGCCTAAT	T ATACTCTCTAATCTTGGC	1	10
- 6789	CATCCTGAACCCATTGAC	ACCACAGCGTGATGGGCT	1	10
- 1164	ATGGTTCGCGGCGGCATT	TTGCGCTTACCCCAACCA	1	50
- 1922	CACTGAATCATGGCTTTA	AGAAGCAATAACCCGCAG	1	50
- 3219	TTCTATTTCTGATGCTGA	GTATCACACACCCCAAAG	1	19
- 3326	TGATGTATTGCTGGTTTC	CTGGTTTTGCGCTTACCC	1	19
- 3360	GATTTCAGAATTAGCCTG	GGGTATCATGTAGCCGCT	1	49
- 3473	GCGGCGTTTGATGTATTG	TGTGGCAGTTGTAGTCCT	1	19
- 3966	TAACTTCCGGAGCCACAC	GAAGACGCGATCTCGCTC	1	17
- 4716	TCCTTTGATGCGAATGCC	GCATAATTACTCCTGATA	1	18
- 5053	AATTCATGGAAAAGGTCT	GCGTAAACTCCGCTGTCA	1	50
- 5244	GTATCAGCAATGTTTATG	GTAGCTTGGCTTCTACCT	1	17
- 6140	ATCGGGGATTCAGTAACA	CGCCTTCTGTCACCACCA	1	10
- 3645	GGTCTGCGTCAAATCCCC	GGTTATCTGTATGTTTTT	1	27
- 3833	AATCGATGGTGTTACCAA	AACCCGGCGCTGAGGCCG	1	57
- 3879	TTGCTGGTTTCTTTCCCG	CTGAGGCCGGGTTATTCT	1	27
- 4014	TTTTCGATGAACTCCGGC	CTTACCGGGTTATCCCCA	1	26
- 4035	CTTCCCAGCCAGCGTTGC	CCTGCACCAGCGTGGTAA	1	27
- 4416	TAAAATAAATCCCCGCGA	TTGGCACATTGGCAGCTA	1	27
- 5194	ATAACTCTGTTGAATGGC	ATATGATGACAATGTCGC	1	58
- 5366	TAACGCAGATCGGATGAT	CCGCCAGTGGCGCACTAT	1	58
- 5905	GGAACAGAGCGGCAATAA	CTGCCTGATTAGCGGCGA	1	25
- 6629	CCGCAATTTCTTTTGTGG	CCTTCAACAAACAAAAAA	1	26
- 4283	TGATGATGCGGGACCAGC	GACCACGCCTTTGGGGCG	1	38
- 6283	TTGCCAGGCTTAAATGAG	ATCTAAGGCCGTCACCTG	1	5
- 1035	ATCACCTTTAAATGCCGT	AACCCCCCGCGATTGGCA	1	15
- 1315	CAGTGCTTTAGCGTTAAC	ATAGCTGTGAAAATATCG	1	45
- 2724	TGCTGGCCCCGTGGCGTT	CTCCAGCCCCTATCCCCC	1	45
- 4318	CCTTTTTCCATGTCGTCT	CAGCGGGTACGGTTGGCG	1	13
- 5146	CGAGAAGATGTTGAGCAA	TCTGCCAGTTCTGCCTCT	1	15
- 5273	GCTGACGCCGCCTTGCCC	CCCGCGATTGGCACATTG	1	14
- 9265	TGTGCCACGCATCATCCC	ATGGATGCAGCCTCCAGA	1	15
- 1373	GTGAGCAATGGTTTCAAC	TGGCGATAGTGGGTATCA	1	23
- 3466	AGGATTCATTGTCCTGCT	GTTCGCCACCCAACCCGC	1	53
- 5445	GTTTAACATGCCGATTGC	AGCGCGCGTAATCCGGCG	1	54
- 5974	ATCCGGATGAAGCCGCTT	GCAATGTATGTCGTTTCA	1	21
- 6666 + 4	GCCGTAAGTCTTGATCTC	CTTA CCTCATCAGTGGCTCTAT	1	22
- 7430	TTTGAATGGTTCGCGGCG	CGTAGCGGTGGAAGTGGC	1	21
- 9265	TTGTGCCACGCATCATCC	ATGGATGCAGCCTCCAGA	1	21
- 3219	GTAATAGCGATGCGTAAT	AGGAAAACAGGAAAGGGG	1	61
- 7081	TCAGCCAGCTTCCCAGCC	GGTGGAAGTGGCGATGAA	1	30

tion of large deletions at a dose rate of 1.5 mGy/h of γ-irradiation.

To further characterize the large deletions induced by the irradiation, we identified the size and junctions of all the 51 deletion mutants (Fig. 4). The size of deletions distributed from 1035 to 9265 bp. About half of the mutants had short homologous sequences up to 11 bp in the junctions while another half had no such short homologous sequences. Two mutants had 1 or 4 bp insertions in the junctions. There was no hot spot of the junctions so that only 2 out of 51 deletions were identified in two mice. There were no obvious differences between large deletions induced by radiation alone and those induced by radiation plus NNK treatments. These results suggest that radiation-induced DSBs in DNA caused large deletions either in the absence or the presence of NNK treatments.

4. Discussion

Humans are exposed to a variety of exogenous and endogenous genotoxic agents. Thus, biological effects of radiation at low doses or low-dose-rate should be evaluated in combination with chemical exposure [12]. In fact, survey of chromosome aberrations in habitats in high-background radiation area in China indicates that cigarette smoking has stronger effects on induction of chromosome aberrations than has the elevated level of natural radiation [23]. Epidemiological studies on underground mineworkers exposed to high levels of radon or plutonium suggest the complexity of interactions between radiation and cigarette smoke in induction of lung tumors [24,25]. Hence, it is important to understand the fundamental mechanisms underlying the interactive genotoxicity and carcinogenicity of cigarette smoking and radiation for the risk assessment on human health.

To elucidate the mechanisms involved, we examined the combined genotoxicity of low-dose-rate γ-irradiation and a tobacco-specific nitrosamine NNK in the lung of *gpt* delta mice. In this study, we focused on whether γ-irradiation would modulate NNK-induced base substitutions and whether NNK treatments would modulate radiation-induced deletions. The mice were irradiated at dose rates of 0.5, 1.0 and 1.5 mGy/h for 22 h for 2 weeks and treated with NNK, i.e., 2 mg/mouse/day for four consecutive days, with irradiation (Fig. 1). The mice were irradiated at the same dose rates for another 2 weeks before sacrifice. Base substitutions and deletions in the lung detected by *gpt* and Spi^- selection, respectively, were analyzed at the molecular levels. We chose the dose rates, i.e., 0.5, 1.0 and 1.5 mGy/h of γ-ray, since Sakai et al. [26] report the suppression of carcinogenicity of 3-methylchoranthrene in ICR female mice by chronic low-dose-rate irradiation of γ-ray at 0.95 mGy/h. According to the report, there is an optimum dose rate of about 1 mGy/h to observe the suppressive effects, and the higher or lower dose rates fail to suppress the tumor induction.

In the present study, NNK treatments significantly enhanced the *gpt* MF (Fig. 2). We observed, however, no modulating effects, i.e., enhancement or suppression, of γ-irradiation at any given dose rate, on the NNK-induced mutations (Fig. 2). This conclusion holds true even when we analyzed the detailed mutation spectra (Table 1). NNK treatments induced similar pattern of base substitutions, i.e., G:C to A:T, G:C to T:A, A:T to T:A and A:T to C:G regardless of the dose rates of combined radiation. In contrast, we observed a suppressive effect of NNK treatments on the radiation-induced deletions. γ-Irradiation enhanced the MF of large deletions in the size of more than 1 kb in a dose-dependent manner (Fig. 3A and Table 2). When combined with NNK treatments, however, the dose–response curve became bell-shaped and the MF at the highest dose rate, i.e., 1.5 mGy/h, was reduced by more than 50% (Fig. 3B and Table 2). The total radiation dose at the highest dose rate was 1.02 Gy. The size of the large deletions was between about 1 and 9 kb, and about half of the large deletions had short homologous sequences in the junctions while other did not (Fig. 4). These features are similar to those of large deletions induced by high dose irradiation with heavy ion, X-ray and γ-ray [20]. Thus, we suggest that NNK induced an adaptive response that eliminated the cells bearing radiation-induced DSBs in DNA.

Previous studies show that low-dose radiation can induce an adaptive response, which causes cells to become resistant to damage by subsequent high doses of radiation [13,27]. Although the exact mechanisms of the adaptive response are not well understood, it is assumed that some proteins are induced by low-dose radiation and they recognize and remove the cells bearing DSB in DNA. Tucker et al. [28] report that the frequency of *Dlb-1* mutations in the small intestine in female F1 mice obtained by crossing SWR/J and C57BL/6 increases along with the total radiation doses of γ-ray, but it saturates and slightly decreases at high doses, i.e., 2–3 Gy (55 mGy/day × 42 or 63 days). Interestingly, our results also suggest that the MFs of the large deletions saturated slightly at the highest dose of 1.02 Gy (Fig. 3A). Thus the adaptive response might be induced slightly at the highest radiation dose even without NNK treatments. Nevertheless, concomitant NNK treatments much clearly suppressed the occurrence of large dele-

tions at the highest radiation dose. We speculate that NNK treatments plus radiation at the highest dose may induce p53-dependent apoptosis, which eliminates the cells bearing radiation-induced DSBs in DNA [29]. The involvement of p53 in the maintenance of genome stability is associated with several pathways such as cell cycle arrest, apoptosis and DNA repair. Low levels of DNA damage appear to enhance p53-dependent DNA repair while high levels induce apoptosis [30]. We envisage that NNK treatments plus radiation at the highest dose introduce genotoxic damage to the cells, the levels of which are enough to trigger the apoptosis. Zhou et al. [31] examined the combined effects of NNK and α-particle irradiation with human–hamster hybrid cultured cells and concluded that the induction of chromosome deletions were additive when the NNK dose was low but a suppressive effect was observed at a higher NNK concentration. In vivo studies also suggest that exposure to high levels of cigarette smoke decrease the risk of lung cancer induced by radon in dogs [32]. However, a multiplicative effect of smoking and radon is observed in rats [33]. In humans, the definitive interaction models have not been established between smoking and radiation exposure [24,25]. Thus, further work is needed to clearly establish the interactive genotoxic mechanisms between radiation and cigarette smoking in vivo.

NNK, a tobacco-specific nitrosamine, is metabolically activated by α-hydroxylation of the methyl and methylene groups [34]. Methylene hydroxylation leads to DNA methylation while methyl hydroxylation leads to pyridyloxobutylated DNA [35]. DNA methylation occurs at N7 and O^6 of guanine and O^4 and O^2 of thymine. It is suggested that O^6-methylguanine (O^6-mG) and pyridyloxobutylated DNA are responsible for G:C to A:T and G:C to T:A mutations, respectively, which activate Ki-*ras* oncogene in the mouse lung tumors induced by NNK [6]. In the present study, G:C to A:T and G:C to T:A mutations were induced by NNK treatments significantly (Table 1). Tiano et al. [36] examined the genotoxicity of NNK in AS52 hamster cells expressing human CYP2A6 and analyzed the induced mutations with the *gpt* gene as a reporter gene for mutations. Because of the lack of O^6-mG methyltransferase in the cell line, about 80% of mutations were G:C to A:T transitions. Interestingly, most of the G:C to A:T transition hotspots occur at the second G of the GGT sequence motif, which is the motif of codon 12 in the Ki-*ras* oncogene [37]. When we define the hotspot as the site where more than four G:C to A:T mutations were identified, we identified 18 hotspots in the *gpt* gene among 155 G:C to A:T mutants recovered from NNK-treated mice. They are nucleotide 27, 64, 86, 87, 92, 107, 110, 113, 115, 116, 128, 274, 281, 287, 402, 409, 417 and 418 when A of ATG of the start codon of the *gpt* gene is set as nucleotide 1. Tiano et al. [36] identified four hotspots of the second G of GGT in nucleotide 23, 116, 128 and 281 in the *gpt* gene, three of which are included in the hotspots identified by us. However, we identified other hotspots such as the second G of GGA at nucleotide 87, 274, 402 and 418, the second G of GGG at nucleotide 27, 64, 92 and 417 and the second G of GGC at nucleotide 113. Thus, we conclude that NNK preferentially induces G:C to A:T mutations at the second G of GGX where X represents any of A, T, G and C. In addition to G:C to A:T and G:C to T:A mutations, we observed an increase in the MFs of A:T to T:A and A:T to C:G in the NNK treated mice (Table 1). Substantial increases in the MFs of A:T to T:A and A:T to C:G are also reported by Hashimoto et al. [38], who examined the genotoxicity of NNK with *lacZ* transgenic mice (Muta^{TM} Mouse). Since reporter genes for mutations, such as *gpt*, *cII* or *lacZ*, are not expressed in vivo and are not imposed by any selection bias, they can reflect any genotoxic events occurring in the genomic DNA. In contrast, oncogenes such as the *ras* gene can only detect mutations that can activate the oncogenic activity of the gene products. Thus, we assume that NNK induces modifications in DNA such as O^4-methyl or O^2-methyl thymine in the lung, which may account for the induction of A:T to C:G and A:T to T:A mutations, respectively [8]. Although the toxicological significance of these mutations is currently unknown, these mutations may contribute to the carcinogenicity of cigarette smoke as well.

γ-Irradiation at dose rate of 1.0 and 1.5 mGy/h clearly enhanced the MFs of large deletions when no NNK treatments were combined (Fig. 3A). The total estimated doses were 0.68 and 1.02 Gy, which may be the lowest radiation doses that gave positive results in transgenic mice mutation assays [16]. In contrast, we could detect no significant increase in the MF of large deletions induced by NNK treatments (Table 2 and Fig. 3A and B). Thus, we suggest that NNK induces mostly base substitutions but not deletions in vivo. Interestingly, NNK treatments induce deletions in cultured mammalian cells. Tiano et al. [36] report that about 20% of mutations induced by NNK treatments are deletions in AS52 hamster cells expressing human CYP2A6. Zhou et al. [31] report that about 80% of NNK-induced mutations are large deletions in the human–hamster hybrid (A_L) cell assay. We speculate that NNK may have a potential to induce both base substitutions and large deletions in vitro but the latter can be eliminated in vivo by the p53-dependent mechanism. Chinese hamster cell lines such as CHO and V79 harbor missense mutation in the *p53*

gene [39,40]. Large deletions might have been detected in the cultured cells because of inefficient p53 functions.

In summary, we have examined the combined genotoxicity of γ-irradiation and NNK treatments in the lung of *gpt* delta mice. Although radiation did not modulate the NNK-induced base substitutions, NNK treatments suppressed the induction of large deletions in size more than 1 kb induced by the irradiation. NNK treatments might induce an adaptive response, which eliminates the cells bearing radiation-induced DSBs in DNA. This finding may be helpful in understanding the molecular mechanisms of genotoxicity as a result of interactions of more than one genotoxic agents in vivo.

Acknowledgements

Part of this study was financially supported by the Budget for Nuclear Research of the Ministry of Education, Culture, Sports, Science and Technology, based on the screening and counseling by the Atomic Energy Commission, and the Tutikawa Memorial Fund for Study in Mammalian Mutagenicity.

References

[1] R. Doll, R. Peto, The causes of cancer: quantitative estimates of avoidable risks of cancer in the United States today, J. Natl. Cancer Inst. 66 (1981) 1191–1308.
[2] Tobacco smoke and involuntary smoking, IARC Monogr Eval. Carcinog. Risk Chem. Hum., vol. 83, International Agency for Research on Cancer, Lyon, France, 2002.
[3] S.S. Hecht, Biochemistry, biology, and carcinogenicity of tobacco-specific *N*-nitrosamines, Chem. Res. Toxicol. 11 (1998) 559–603.
[4] S.S. Hecht, Tobacco carcinogens, their biomarkers and tobacco-induced cancer, Nat. Rev. Cancer 3 (2003) 733–744.
[5] International Agency for Research on Cancer Press Release, vol. 154, International Agency for Research on Cancer, Lyon, France, 2004.
[6] Z.A. Ronai, S. Gradia, L.A. Peterson, S.S. Hecht, G to A transitions and G toT transversions in codon 12 of the Ki-*ras* oncogene isolated from mouse lung tumors induced by 4-(methylnitrosamino)-1-(3-pyridyl)-1-butanone (NNK) and related DNA methylating and pyridyloxobutylating agents, Carcinogenesis 14 (1993) 2419–2422.
[7] R. Guza, M. Rajesh, Q. Fang, A.E. Pegg, N. Tretyakova, Kinetics of O^6-methyl-2′-deoxyguanosine repair by O^6-alkylguanine DNA alkyltransferase within *K-ras* gene-derived DNA sequences, Chem. Res. Toxicol. 19 (2006) 531–538.
[8] E.C. Friedberg, G.C. Walker, W. Siede, R.D. Wood, R.A. Schultz, T. Ellenberger, DNA Repair and Mutagenesis, 2nd ed., ASM Press, Washington, DC, 2006, pp. 1–1118.
[9] United Nations Scientific Committee on the Effects of Atomic Radiation, Sources, Effects and Risks of Ionising Radiation, 1988 Report to the General Assembly with Annexes, United Nations Press, New York, 1989.
[10] J.H. Lubin, K. Steindorf, Cigarette use and the estimation of lung cancer attributable to radon in the United States, Radiat. Res. 141 (1995) 79–85.
[11] H.P. Leenhouts, M.J. Brugmans, Calculation of the 1995 lung cancer incidence in The Netherlands and Sweden caused by smoking and radon: risk implications for radon, Radiat. Environ. Biophys. 40 (2001) 11–21.
[12] United Nations Scientific Committee on the Effects of Atomic Radiation, Combined Effects of Radiation and Other Agents, Report to the General Assembly, United Nations Press, New York, 1998.
[13] M.S. Sasaki, Y. Ejima, A. Tachibana, T. Yamada, K. Ishizaki, T. Shimizu, T. Nomura, DNA damage response pathway in radioadaptive response, Mutat. Res. 504 (2002) 101–118.
[14] T. Lindahl, B. Sedgwick, M. Sekiguchi, Y. Nakabeppu, Regulation and expression of the adaptive response to alkylating agents, Annu. Rev. Biochem. 57 (1988) 133–157.
[15] N.G. Oliveira, M. Neves, A.S. Rodrigues, G.O. Monteiro, T. Chaveca, J. Rueff, Assessment of the adaptive response induced by quercetin using the MNCB peripheral blood human lymphocytes assay, Mutagenesis 15 (2000) 77–83.
[16] T. Nohmi, K.I. Masumura, *gpt* Delta transgenic mouse: a novel approach for molecular dissection of deletion mutations in vivo, Adv. Biophys. 38 (2004) 97–121.
[17] T. Nohmi, T. Suzuki, K. Masumura, Recent advances in the protocols of transgenic mouse mutation assays, Mutat. Res. 455 (2000) 191–215.
[18] M. Miyazaki, H. Yamazaki, H. Takeuchi, K. Saoo, M. Yokohira, K. Masumura, T. Nohmi, Y. Funae, K. Imaida, T. Kamataki, Mechanisms of chemopreventive effects of 8-methoxypsoralen against 4-(methylnitrosamino)-1-(3-pyridyl)-1-butanone-induced mouse lung adenomas, Carcinogenesis 26 (2005) 1947–1955.
[19] T. Nohmi, M. Suzuki, K. Masumura, M. Yamada, K. Matsui, O. Ueda, H. Suzuki, M. Katoh, H. Ikeda, T. Sofuni, Spi$^-$ selection: an efficient method to detect gamma-ray-induced deletions in transgenic mice, Environ. Mol. Mutagen. 34 (1999) 9–15.
[20] K. Masumura, K. Kuniya, T. Kurobe, M. Fukuoka, F. Yatagai, T. Nohmi, Heavy-ion-induced mutations in the *gpt* delta transgenic mouse: comparison of mutation spectra induced by heavy-ion, X-ray, and gamma-ray radiation, Environ. Mol. Mutagen. 40 (2002) 207–215.
[21] T. Nohmi, K. Masumura, Molecular nature of intrachromosomal deletions and base substitutions induced by environmental mutagens, Environ. Mol. Mutagen. 45 (2005) 150–161.
[22] M. Horiguchi, K.I. Masumura, H. Ikehata, T. Ono, Y. Kanke, T. Nohmi, Molecular nature of ultraviolet B light-induced deletions in the murine epidermis, Cancer Res. 61 (2001) 3913–3918.
[23] W. Zhang, C. Wang, D. Chen, M. Minamihisamatsu, H. Morishima, Y. Yuan, L. Wei, T. Sugahara, I. Hayata, Effect of smoking on chromosomes compared with that of radiation in the residents of a high-background radiation area in China, J. Radiat. Res. (Tokyo) 45 (2004) 441–446.
[24] Z.B. Tokarskaya, B.R. Scott, G.V. Zhuntova, N.D. Okladnikova, Z.D. Belyaeva, V.F. Khokhryakov, H. Schollnberger, E.K. Vasilenko, Interaction of radiation and smoking in lung cancer induction among workers at the Mayak nuclear enterprise, Health Phys. 83 (2002) 833–846.
[25] V.E. Archer, Enhancement of lung cancer by cigarette smoking in uranium and other miners, Carcinog. Compr. Surv. 8 (1985) 23–37.

[26] K. Sakai, Y. Hoshi, T. Nomura, T. Oda, T. Iwasaki, K. Fujita, T. Yamada, H. Tanooka, Suppression of carcinogenic processes in mice by chronic low dose rate gamma-irradiation, Int. J. Low Radiat. 1 (2003) 142–146.
[27] S. Wolff, Failla memorial lecture. Is radiation all bad? The search for adaptation, Radiat. Res. 131 (1992) 117–123.
[28] J.D. Tucker, K.J. Sorensen, C.S. Chu, D.O. Nelson, M.J. Ramsey, C. Urlando, J.A. Heddle, The accumulation of chromosome aberrations and *Dlb-1* mutations in mice with highly fractionated exposure to gamma radiation, Mutat. Res. 400 (1998) 321–335.
[29] C.E. Canman, M.B. Kastan, Role of p53 in apoptosis, Adv. Pharm. 41 (1997) 429–460.
[30] H. Offer, N. Erez, I. Zurer, X. Tang, M. Milyavsky, N. Goldfinger, V. Rotter, The onset of p53-dependent DNA repair or apoptosis is determined by the level of accumulated damaged DNA, Carcinogenesis 23 (2002) 1025–1032.
[31] H. Zhou, L.X. Zhu, K. Li, T.K. Hei, Radon, tobacco-specific nitrosamine and mutagenesis in mammalian cells, Mutat. Res. 430 (1999) 145–153.
[32] F.T. Cross, R.F. Palmer, R.E. Filipy, G.E. Dagle, B.O. Stuart, Carcinogenic effects of radon daughters, uranium ore dust and cigarette smoke in beagle dogs, Health Phys. 42 (1982) 33–52.
[33] F.T. Cross, Radioactivity in cigarette smoke issue, Health Phys. 46 (1984) 205–208.
[34] S.S. Hecht, D. Hoffmann, Tobacco-specific nitrosamines, an important group of carcinogens in tobacco and tobacco smoke, Carcinogenesis 9 (1988) 875–884.
[35] Y. Lao, P.W. Villalta, S.J. Sturla, M. Wang, S.S. Hecht, Quantitation of pyridyloxobutyl DNA adducts of tobacco-specific nitrosamines in rat tissue DNA by high-performance liquid chromatography-electrospray ionization-tandem mass spectrometry, Chem. Res. Toxicol. 19 (2006) 674–682.
[36] H.F. Tiano, R.L. Wang, M. Hosokawa, C. Crespi, K.R. Tindall, R. Langenbach, Human CYP2A6 activation of 4-(methylnitrosamino)-1-(3-pyridyl)-1-butanone (NNK): mutational specificity in the *gpt* gene of AS52 cells, Carcinogenesis 15 (1994) 2859–2866.
[37] L.A. Peterson, S.S. Hecht, O^6-Methylguanine is a critical determinant of 4-(methylnitrosamino)-1-(3-pyridyl)-1-butanone tumorigenesis in A/J mouse lung, Cancer Res. 51 (1991) 5557–5564.
[38] K. Hashimoto, K. Ohsawa, M. Kimura, Mutations induced by 4-(methylnitrosamino)-1-(3-pyridyl)-1-butanone (NNK) in the *lacZ* and *cII* genes of Muta Mouse, Mutat. Res. 560 (2004) 119–131.
[39] H. Lee, J.M. Lamer, J.L. Hamlin, Cloning and characterization of Chinese hamster p53 cDNA, Gene 184 (1997) 177–183.
[40] W. Chaung, L.J. Mi, R.J. Boorstein, The p53 status of Chinese hamster V79 cells frequently used for studies on DNA damage and DNA repair, Nucl. Acids Res. 25 (1997) 992–994.


R00126313_MUTGEN_401179

Enhanced Spontaneous and Benzo(*a*)pyrene-Induced Mutations in the Lung of Nrf2-Deficient *gpt* Delta Mice

Yasunobu Aoki,[1] Akiko H. Hashimoto,[1] Kimiko Amanuma,[1] Michi Matsumoto,[1] Kyoko Hiyoshi,[1,2] Hirohisa Takano,[1] Ken-ichi Masumura,[4] Ken Itoh,[3] Takehiko Nohmi,[4] and Masayuki Yamamoto[3]

[1]Research Center for Environmental Risk, National Institute for Environmental Studies; [2]Graduate School of Comprehensive Human Sciences; [3]Center for TARA and ERATO-JST, University of Tsukuba, Ibaraki, Japan; and [4]Division of Genetics and Mutagenesis, National Institute of Health Sciences, Tokyo, Japan

Abstract

The lung is an organ that is sensitive to mutations induced by chemicals in ambient air, and transgenic mice harboring guanine phosphoribosyltransferase (*gpt*) gene as a target gene are a well-established model system for assessing genotoxicity *in vivo*. Transcription factor Nrf2 mediates inducible and constitutive expression of cytoprotective enzymes against xenobiotics and mutagens. To address whether Nrf2 is also involved in DNA protection, we generated *nrf2*$^{+/-}$*::gpt* and *nrf2*$^{-/-}$*::gpt* mice. The spontaneous mutation frequency of the *gpt* gene in the lung was approximately three times higher in *nrf2*-null (*nrf2*$^{-/-}$) mice than *nrf2* heterozygous (*nrf2*$^{+/-}$) and wild-type (*nrf2*$^{+/+}$) mice, whereas in the liver, the mutation frequency was higher in *nrf2*$^{-/-}$ and *nrf2*$^{+/-}$ mice than in *nrf2*$^{+/+}$ wild-type mice. By contrast, no difference in mutation frequency was observed in testis among the three genotypes. A single intratracheal instillation of benzo(*a*)pyrene (BaP) increased the lung mutation frequency 3.1- and 6.1-fold in *nrf2*$^{+/-}$ and *nrf2*$^{-/-}$ mice, respectively, compared with BaP-untreated *nrf2*$^{+/-}$ mice, showing that *nrf2*$^{-/-}$ mice are more susceptible to genotoxic carcinogens. Surprisingly, mutation profiles of the *gpt* gene in BaP-treated *nrf2*$^{+/-}$ mice was substantially different from that in BaP-untreated *nrf2*$^{-/-}$ mice. In *nrf2*$^{-/-}$ mice, spontaneous and BaP-induced mutation hotspots were observed at nucleotides 64 and 140 of *gpt*, respectively. These results thus show that Nrf2 aids in the prevention of mutations *in vivo* and suggest that Nrf2 protects genomic DNA against certain types of mutations. [Cancer Res 2007;67(12):5643–8]

Introduction

Nrf2 is an essential transcription factor for inducible and constitutive expression of several phase II detoxification enzymes, including glutathione *S*-transferase-α (GST-α) and GST-π and UDP-glucuronosyl transferase 1A6 (1). Nrf2 also regulates the expression of antioxidant enzymes, including NAD(P)H:quinone oxidoreductase-1 and heme oxygenase-1, in response to oxidative stress (2, 3). Keap1 acts to harness Nrf2 to the cytoplasm, and Nrf2 in this complex rapidly undergoes ubiquitination and proteasomal degradation via Keap1-Cullin 3 E3 interactions (4). However, oxidative or electrophilic modification of Keap1 triggers Nrf2 stabilization (5, 6). During oxidative conditions, Nrf2 translocates into the nucleus and activates cytoprotective gene expression by heterodimerizing with small Maf family members and binding to antioxidant-responsive elements (ARE) or electrophile-responsive element in regulatory regions of cytoprotective genes.

Nrf2-mediated induction of cytoprotective enzymes plays an important role in mitigating the adverse effects of mutagens and oxidants. In Nrf2-deficient mice, which have attenuated basal and inducible expression of these enzymes (7): (*a*) DNA adduct formation is accelerated after diesel exhaust exposure (8); (*b*) hepatotoxicity is enhanced after acetaminophen administration (9); and (*c*) benzo(*a*)pyrene (BaP)–induced DNA adduct and neoplasm formation in forestomach is more prevalent than in wild-type mice (10, 11). Taken together, Nrf2 attenuation or malfunction may be an important aspect of diseases caused by environmental mutagens or oxidants, although the mechanism linking Nrf2 deficiency and mutation frequency is not well understood.

Transgenic guanine phosphoribosyltransferase (*gpt*) delta mice are a model system for detecting *in vivo* mutations (12). In this mouse system, the *gpt* gene is integrated into the genome as a target gene for detecting mutations, and when the *gpt* gene is rescued from genomic DNA to *Escherichia coli*, *gpt* mutants can be randomly selected as rescued *E. coli* colonies that form on plates containing 6-thioguanine (6-TG). To assess whether Nrf2 deficiency increases the mutational risk following exposure to BaP, the current study uses *nrf2*$^{-/-}$*::gpt* mice to analyze mutagenic activity *in vivo*. Furthermore, alterations in the mutation spectrum between *nrf2*$^{+/-}$ and *nrf2*$^{-/-}$ mice were assessed after exposure to BaP.

Materials and Methods

Mice. C57BL/6J *nrf2* knockout mice (7) and *gpt* delta mice (C57BL/6J background; ref. 12) were as described previously, and *gpt* mice were obtained from Japan SLC. Nrf2-deficient mice (*nrf2*$^{-/-}$) were crossed with *gpt* delta transgenic mice (*nrf2*$^{+/+}$*::gpt/gpt*), and the resultant F1 mice (*nrf2*$^{+/-}$*::gpt/0*) were crossed again with Nrf2-deficient mice (*nrf2*$^{-/-}$) to produce *nrf2* knockout *gpt* mice that are homozygous (*nrf2*$^{-/-}$) or heterozygous (*nrf2*$^{+/-}$) to the *nrf2* knockout allele (*nrf2*$^{+/-}$*::gpt* and *nrf2*$^{-/-}$*::gpt*, respectively). Genotyping for *nrf2* was accomplished by PCR amplification of genomic DNA isolated from tails. PCR primers were as follows: 5′-TGGACGGGACTATTGAAGGCTG-3′ (sense for both genotype) and 5′-GCCGCCTTTTCAGTAGATGGAGG-3′ (antisense for wild-type mice) and 5′-GCGGATTGACCGTAATGGGATAGG-3′ (antisense for *LacZ*). The presence of the *gpt* transgene was confirmed by PCR as previously described (12). Nine male Nrf2-deficient *gpt* delta mice (*nrf2*$^{-/-}$*::gpt*) and nine male heterozygous *nrf2* knockout *gpt* delta mice (*nrf2*$^{+/-}$*::gpt*), both 7 to 9 weeks old, were obtained from this breeding scheme. Experiments

Note: Supplementary data for this article are available at Cancer Research Online (http://cancerres.aacrjournals.org/).

Y. Aoki and A.H. Hashimoto contributed equally to this work.

Requests for reprints: Yasunobu Aoki, National Institute for Environmental Studies, 16-2 Onogawa, Tsukuba, Ibaraki 305-8506, Japan. Phone: 81-29-850-2390; Fax: 81-29-850-2588; E-mail: ybaoki@nies.go.jp.

doi:10.1158/0008-5472.CAN-06-3355

were done according to protocols approved by the Institutional Animal Care and Use Committee at National Institute for Environmental Studies.

Mouse treatment. BaP (Wako Pure Chemical) was dissolved in tricaprylin $[CH_3(CH_2)_6COOCH_2]_2CHOCO(CH_2)_6CH_3$ (Sigma-Aldrich). Five *nrf2*$^{+/-}$::*gpt* mice and four *nrf2*$^{-/-}$::*gpt* mice were treated with 1 mg BaP dissolved in 50 μL tricaprylin given in a single intratracheal instillation under anesthesia with halothane for mutation analysis as previously reported (13). Vehicle (50 μL tricaprylin) was given to five *nrf2*$^{+/-}$::*gpt* mice and four *nrf2*$^{-/-}$::*gpt* mice as BaP-untreated groups. For immunoblot analysis, three *nrf2*$^{+/-}$ or *nrf2*$^{-/-}$ mice were used for each group. Mice were sacrificed 1 and 14 days after BaP administration under anesthesia with ethyl ether for Western blotting and mutation analysis, respectively. Lungs were removed, quickly frozen in liquid nitrogen, and stored at −80°C until the DNA was isolated.

***gpt* mutation assay.** Genomic DNA was extracted from the lungs using the RecoverEase DNA Isolation kit (Stratagene). Lambda EG10 phages were recovered from the genomic DNA using Transpack Packaging Extract (Stratagene). *E. coli* (YG6020 expressing Cre recombinase) were infected with the recovered phage harboring the *gpt* gene and the chloramphenicol (Cm) acethyltransferase (*cat*) gene (a selection marker), and these genes were rescued as a plasmid (14). The *gpt* mutants can be detected as colonies arising on plates containing Cm and 6-TG. The bacteria were then spread onto M9 salts plates containing Cm and 6-TG, which were incubated for 72 h at 37°C for selection of the colonies harboring a plasmid carrying a mutated *gpt* gene and *cat* gene. The 6-TG–resistant colonies were streaked onto selection plates for confirmation of the resistant phenotype. The cells were then cultured in Luria-Bertani broth containing 25 μg/mL of Cm at 37°C and collected by centrifugation. The bacterial pellets were stored at −80°C until DNA sequencing analysis was done. Mutant frequencies for the *gpt* gene were calculated by dividing the number of colonies growing on (M9 + Cm + 6-TG) agar plates by the number of colonies growing on (M9 + Cm) agar plates, which is the number of colonies harboring the plasmid. To ensure determination of the mutant frequency, mutant colonies were selected from over 300,000 colonies (15).

PCR and DNA sequencing analysis of 6-TG–resistant mutants. A 739-bp DNA fragment containing the *gpt* gene was amplified by PCR using primer 1 and primer 2, as described previously (13). The reaction mixture contained 5 pmol of each primer and 200 mmol/L of each deoxynucleotide triphosphate. PCR amplification was carried out using Ex Taq DNA polymerase (Takara Bio) and done with a Model PTC-100 Thermal Cycler (MJ Research). After the PCR products were purified, sequencing reactions were done by using a DYEnamic ET Terminator kit (Amersham Biosciences). The sequencing primers (primer A and primer C) were as described previously (13).

Immunoblot analysis of GSTs. Frozen lung was homogenized with 2 mL of 50 mmol/L HEPES buffer (pH 7.5) containing 150 mmol/L NaCl, 1 mmol/L DTT, and 0.2 mmol/L phenylmethylsulfonyl fluoride by glass-Teflon homogenizer chilled with ice. The homogenates were subjected to two steps of centrifugation at 4°C (15,000 × *g* for 15 min followed by 100,000 × *g* for 60 min) according to Chanas et al. (16). Resulting 100,000 × *g* supernatants (cytosol fractions) were stored at −80°C until use. After the cytosol fractions mixed with sample buffer containing 1% SDS were heated at 95°C, 9 μg protein (for detecting GST A1/2) or 3 μg protein (for detecting GST A3 and GST P1/2) from each sample was subjected to SDS-PAGE with 15% polyacrylamide gel (17). Proteins separated on the gel were transferred to Immobilon-P membrane (Amersham Biosciences). GST A1/2, GST A3 (18–20), and GST P1/2 were immunochemically detected using anti-mouse GST A1/2 and A3 rabbit sera (kindly provided by Dr. J.D. Hayes, University of Dundee, United Kingdom) and GST P1/2 rabbit serum (kindly provided by Dr. I. Hatayama, Aomori Prefecture Institute of Public Health and Environment, Japan), respectively, and goat anti-rabbit IgG antibody labeled with horseradish peroxidase (16). ECL-plus and Typhoon 9400 BioImage analyzer (Amersham Biosciences) were used to visualize bands.

Statistical analysis. All data are expressed as mean ± SD. Statistical significance of mutant frequency was evaluated using the Student's *t* test. $P < 0.05$ was considered statistically significant. Statistical comparisons of mutational spectra were done using the Adams-Skopek test (21).

Results and Discussion

The frequency of spontaneous mutations in the lung, liver, and testis was compared among *gpt* delta mice (*nrf2*$^{+/+}$), heterozygous mice (*nrf2*$^{+/-}$), and homozygous mice (*nrf2*$^{-/-}$). In the lung and liver, the mutation frequency was significantly elevated in *nrf2*$^{-/-}$ mice, compared with *nrf2*$^{+/+}$ mice (Fig. 1*A*; Supplementary Table S1). The mutant frequency in the lung was approximately three times higher in *nrf2*$^{-/-}$ mice ($1.40 \pm 0.28 \times 10^{-5}$) than *nrf2*$^{+/-}$ and *nrf2*$^{+/+}$ mice ($0.48 \pm 0.05 \times 10^{-5}$ and $0.50 \pm 0.16 \times 10^{-5}$, respectively), whereas the mutant frequency was significantly higher in both *nrf2*$^{-/-}$ and *nrf2*$^{+/-}$ mice ($1.24 \pm 0.13 \times 10^{-5}$ and $1.47 \pm 0.15 \times 10^{-5}$, respectively) than *nrf2*$^{+/+}$ mice in liver ($0.72 \pm 0.24 \times 10^{-5}$). In contrast, no difference in mutation frequency was observed in testis among the three genotypes (Fig. 1*A*). Whereas

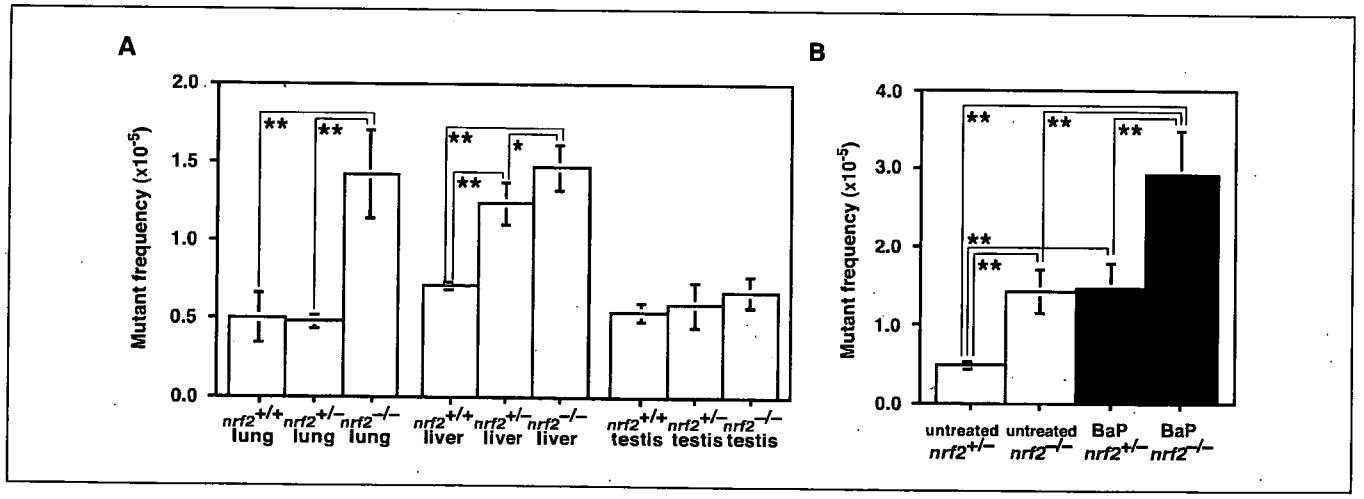

Figure 1. The mutant frequency of 6-TG selection (*A*) in the lung, liver, and testis of *gpt* delta mice (*nrf2*$^{+/+}$, *yellow column*, $n = 3$), and *nrf2*$^{+/-}$ (*light blue column*, $n = 5$) and *nrf2*$^{-/-}$ (*pink column*, $n = 4$) *gpt* delta mice and (*B*) in the lungs of *nrf2*$^{+/-}$ (*blue column*, $n = 5$) and *nrf2*$^{-/-}$ (*red column*, $n = 4$) *gpt* delta mice after BaP treatment. Data of *nrf2*$^{+/-}$ and *nrf2*$^{-/-}$ lungs in (*A*) are replicated as BaP-untreated *nrf2*$^{+/-}$ and *nrf2*$^{-/-}$, respectively, in (*B*). *Columns*, mean; *bars*, SD. *, $P < 0.05$; **, $P < 0.01$, statistical significance among the groups was determined using the Student's *t* test.